The Journal of Neuroscience, October 1994, 14(10): 6021–6032

Glutamate in Thalamic Fibers Terminating in Layer IV of Primary Sensory Cortex

Viktor N. Kharazia and Richard J. Weinberg

Department of Cell Biology and Anatomy, University of North Carolina, Chapel Hill, North Carolina 27599

Biochemical and pharmacological experiments support glutamate (Glu) as a thalamocortical transmitter, but do not distinguish direct from indirect effects (via excitation of glutamergic corticocortical fibers); anatomical studies to date have yielded variable results. We identified thalamocortical terminals in layer IV of primary somatic sensory, auditory, and visual cortex by injecting WGA-HRP in the corresponding thalamic sensory relay nuclei of rats. Terminals from each thalamic nucleus were similar, containing abundant mitochondria and loosely packed clear vesicles; they made asymmetric synaptic contacts mainly with dendritic spines. After tracer injections into nearby regions of cortex, most terminals also made asymmetric contacts mainly onto spines, but these corticocortical terminals were smaller, containing sparse mitochondria and densely packed clear vesicles. GABAergic terminals (identified by postembedding immunogold staining) made symmetric synapses mainly onto dendritic shafts; those terminating near thalamocortical terminals were also large and contained abundant mitochondria. To determine whether Glu is enriched in thalamocortical terminals, we performed postembedding double-labeling immunocytochemistry for Glu and GABA, using different gold particle sizes. The density of particles coding for Glu was significantly enriched over identified thalamocortical terminals, in comparison to nearby dendrites, astrocytes, and GABAergic terminals, and this enrichment was similar for all three sensory areas. The degree of enrichment in thalamocortical terminals, but not in GABAergic terminals, was linearly related to vesicle density. We conclude that Glu is likely to be a neurotransmitter for thalamocortical relay neurons.

[Key words: somatic, visual, auditory, GABA, ultrastructure, anterograde tracing, postembedding immunocytochemistry]

The neocortex is a laminated structure; variations in thickness, organization, and cellular composition of its layers are related to functional specialization (Kemper and Galaburda, 1984). Primary sensory cortex is characterized by an especially prominent internal granular layer (layer IV; Brodmann, 1909). Neurons in this layer receive direct synaptic input from specific sensory nuclei of the thalamus and thus represent the first stage of cortical processing of sensory information (Herkenham, 1980, 1986; Jones, 1981, 1985).

In view of these common features, terminals from specific thalamic nuclei to layer IV of sensory cortex may be morphologically homogeneous and use the same neurotransmitter irrespective of the sensory modality. However, each modality has specific processing requirements; for example, synaptic processing in auditory cortex has uniquely stringent temporal constraints, as auditory localization requires detection of very small binaural timing differences. Such requirements raise the possibility that the terminals of thalamocortical axons from the different sensory relay nuclei are morphologically and neurochemically distinct. These terminals are likely to be excitatory, but their neurotransmitter remains unidentified (Jones, 1985, 1988).

A variety of pharmacological, electrophysiological, and biochemical evidence supports a role for glutamate (Glu) as a transmitter in thalamocortical fibers to primary sensory areas (reviewed by Tsumoto, 1990; Hicks et al., 1991). However, the likelihood that Glu is a major transmitter in corticocortical pathways (Streit, 1984; Conti et al., 1987, 1989; Giuffrida and Rustioni, 1989; McCormick, 1992; Orrego and Villanueva, 1993) complicates interpretation of this evidence: release of Glu associated with thalamic stimulation, interpreted as originating from thalamocortical terminals, might instead represent indirect activation of intracortical synapses. Similarly, the demonstration that Glu antagonists block thalamic activation, though consistent with Glu as a thalamocortical transmitter, might alternatively reflect an indirect or tonic effect of intracortical excitatory connections.

Previous anatomical studies using ^{3}H-D-Asp as a retrograde tracer for putative glutamergic thalamocortical neurons in the ventrobasal and lateral geniculate nuclei provide equivocal support for Glu as a thalamocortical transmitter (Ottersen et al., 1983; Barbaresi et al., 1987; Johnson and Burkhalter, 1992). Immunocytochemical investigation has demonstrated that relay neurons in thalamus stain for Glu, as well as aspartate (Rustioni et al., 1988). In view of the numerous metabolic functions of glutamate, somatic staining is less conclusive than demonstration of Glu enrichment in synaptic terminals. Moreover, thalamocortical relay neurons are also immunopositive for *N*-acetylaspartylglutamate, another candidate for transmitter in thalamocortical fibers (Tieman et al., 1991; Xing and Tieman, 1993). Montero (1990) demonstrated Glu enrichment in local axon collaterals of relay neurons in the lateral geniculate nucleus, suggesting that cortical terminals of these neurons may also be enriched in Glu. In a preliminary report, we demonstrated Glu enrichment in thalamic terminals to S-1 (Kharazia and

Received Nov. 22, 1993; revised Mar. 4, 1994; accepted Apr. 7, 1994.

We gratefully acknowledge the contribution of K. Phend for histological assistance. We thank A. Rustioni for his support and assistance in this project, and T. P. Hicks, F. Conti, and C. G. Cusick for their careful critiques of the manuscript. This research was supported by NIH Grant NS-29879 (to R.J.W.).

Correspondence should be addressed to Viktor Kharazia, Department of Cell Biology and Anatomy, CB # 7090, University of North Carolina, Chapel Hill, NC 27599.

Copyright © 1994 Society for Neuroscience 0270-6474/94/146021-12$05.00/0

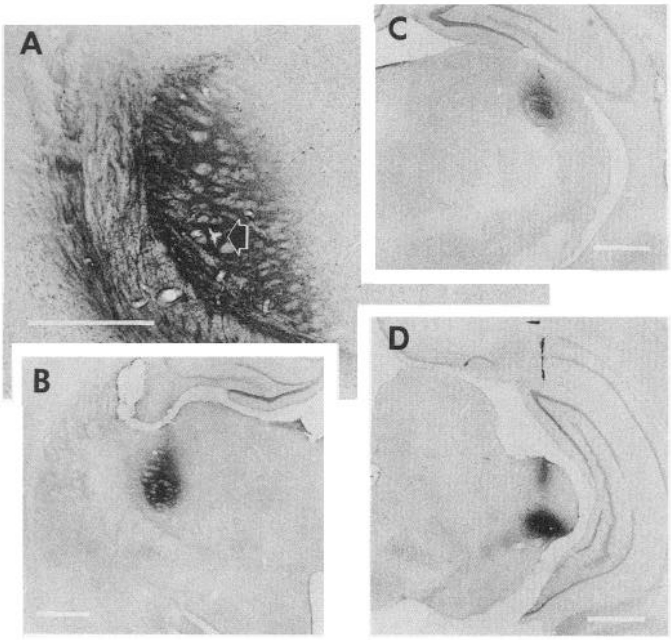

Figure 1. Injection sites, in coronal sections through the thalamus, processed with diaminobenzidine histochemistry. *A*, Large injection site after pressure injection of WGA-HRP in ventrobasal complex (*arrow* shows needle track). Tracer also entered reticular thalamic nucleus. Note much more circumscribed injection sites after iontophoresis of WGA-HRP into VPL (*B*), dorsal lateral geniculate (*C*), and ventral medial geniculate (*D*). Scale bars, 1 mm.

Weinberg, 1993), using an antibody that exhibits minimal cross-reactivity with aspartate or *N*-acetylaspartylglutamate (Abdullah et al., 1992). By combining postembedding immunocytochemistry at the electron microscopic level with anterograde transport to identify thalamic fibers terminating in primary somatic sensory, auditory, and visual cortex, we now report that thalamocortical terminals for all three sensory systems have similar morphologies and similar degrees of Glu enrichment.

Materials and Methods

Surgery and tissue preparation. All surgical procedures were performed according to protocols approved by the local Institutional Animal Care and Use Committee. Thirteen male Sprague–Dawley rats were used for stereotaxic injections into thalamus (Paxinos and Watson, 1986). Animals were anesthetized with sodium pentobarbital (50 mg/kg, i.p.) and injected with wheat germ agglutinin conjugated to horseradish peroxidase (WGA-HRP; Sigma). Small iontophoretic injections (2–5 μA, 3–5 min) of 1% WGA-HRP in water were placed in the ventral posterolateral (VPL) or ventral posteromedial (VPM) nuclei, the dorsal lateral geniculate nucleus, or the ventral part of the medial geniculate nucleus, using a vertical approach (Fig. 1*B–D*). To obtain anterograde labeling from both VPM and VPL, pressure delivery was preferable to iontophoresis. Pressure injections were made into the ventrobasal complex with 0.5–1 μl of 2% WGA-HRP diluted in 2% dimethyl sulfoxide, using an oblique 45° approach through occipital cortex (Fig. 1*A*).

In a preliminary study, we found that labeled thalamic terminals in S-1 were morphologically distinct from a second common type, which we tentatively identified as corticocortical (Kharazia and Weinberg, 1993). To assess whether this second class of terminals is indeed corticocortical (rather than, e.g., a type of thalamocortical terminal that fails to transport WGA-HRP), iontophoretic injections of WGA-HRP or pressure injections of HRP conjugated to the B subunit of cholera toxin (CTB-HRP; List; 0.2% in 2% DMSO) were made in layers IV–VI of ipsilateral sensory cortex.

After 48 hr survival, animals were deeply anesthetized with sodium pentobarbital (80 mg/kg) and perfused with 100 ml of heparinized normal saline, followed by 500 ml of a mixture of 2.5% glutaraldehyde, 0.5–1% paraformaldehyde, and 0.2% picric acid in 0.1 M phosphate buffer, pH 7.4. The brains were removed, postfixed for 1–2 hr in the same fixative, and stored in phosphate buffer at 4°C. Thick coronal sections (50 μm) were cut on a Vibratome and collected in phosphate buffer.

Sections were reacted with diaminobenzidine to verify injection sites. Sections including relevant regions of cortex were reacted according to a tetramethylbenzidine/tungstate (TMB/W) protocol to visualize peroxidase (Weinberg and Van Eyck, 1991). In one case, cortex was flattened and tangential sections through S-1 were also reacted for TMB/W. Sections for light microscopy (LM) were usually reacted in TMB for 40–60 min and stained with thionin. For electron microscopy (EM), sections of cortex were reacted 10–15 min, stabilized with diaminobenzidine, immersed for 1 hr in 1% osmium tetroxide in phosphate buffer, pH 6, stained for 1 hr in 1% uranyl acetate in maleate buffer, and wafer embedded in Epon-Spurr resin.

Immunocytochemistry. Thin sections including layer IV were collected on uncoated 300 mesh nickel grids and immunostained for Glu as previously described (Phend et al., 1992). Briefly, grids were washed with TRIS-buffered saline containing 0.3% Triton X-100 (TBST), pH 7.6, incubated overnight in primary antibody (anti-Glu #482a, Arnel; 1:100,000–1:500,000 in TBST plus 1 mM aspartate), rinsed in TBST, pH 7.6, transferred to TBST, pH 8.2, incubated in secondary antibody (goat anti-rabbit IgG conjugated to gold particles from Amersham, E-Y, or Jackson; 1:25 in TBST, pH 8.2) for 1 hr, rinsed, and dried. To control for the specificity of immunoreaction, we (1) substituted preimmune rabbit serum for primary antibody, and (2) preincubated primary antibody with Glu (0.01–10 mM) before use. To help provide a reference for "background" Glu staining (as explained below) most of the material was also stained for GABA, using different sizes of gold particles (Phend et al., 1992): after staining for Glu, grids were kept for 1 hr over paraformaldehyde vapors at 80°C (to deactivate remaining binding sites) and processed according to the same protocol using an antibody to GABA (Arnel; 1:5000–10,000). Grids were counterstained with 1% uranyl acetate and Sato's lead, and examined at 80 kV in a JEOL 200CX electron microscope.

Data analysis. Material was randomly scanned at 20,000×; whenever a terminal containing anterograde labeling was seen, it was photographed. Typically, for each animal, two blocks were cut from each of two wafers (prepared from sections several hundred micrometers apart), and four grids were examined from each block. Photomicrographs were usually printed at a final magnification of 35,000×. Morphometric analysis and determination of particle density were performed on all photomicrographs for which membrane definition was satisfactory, and the labeled terminal was not completely obscured by crystals of HRP reaction product. Areas of labeled thalamocortical terminals, dendrites postsynaptic to them, randomly selected GABA-negative dendrites, GABA-labeled terminals, and astrocytic profiles (identified according to criteria of Peters et al., 1991) were measured on a data tablet interfaced to a IBM PC. Gold particles over measured profiles were counted, and particle densities for each profile were computed using a spreadsheet program. Mitochondria were considered separately. In one animal with especially good tissue preservation, synaptic vesicles were counted. Statistical significance was assessed using one-way ANOVA, two-sided *t* tests, and regression analysis; means are reported ± standard errors.

Results

Light microscopy

Injections in thalamic relay nuclei resulted in labeling in the corresponding area of primary sensory cortex (Fig. 2). Retrograde labeling was prominent in layer VI, extending into layer V. TMB/W crystals interpreted as anterograde labeling were concentrated in layer IV; labeling also extended into more superficial layers (Fig. 3*A*). Probable anterograde labeling in layer VI was masked by the numerous retrogradely labeled corticothalamic neurons. Anterograde labeling in S-1 was patchy in both coronal and tangential planes of section (Fig. 3*B,C*). After comparable iontophoretic injections, anterograde labeling was denser in S-1 than in A-1 or V-1. Vertical pairing of anterograde labeling in layer IV with retrograde labeling in layers V–VI was typical but not invariable; in some cases anterograde labeling was much stronger than retrograde, or vice versa.

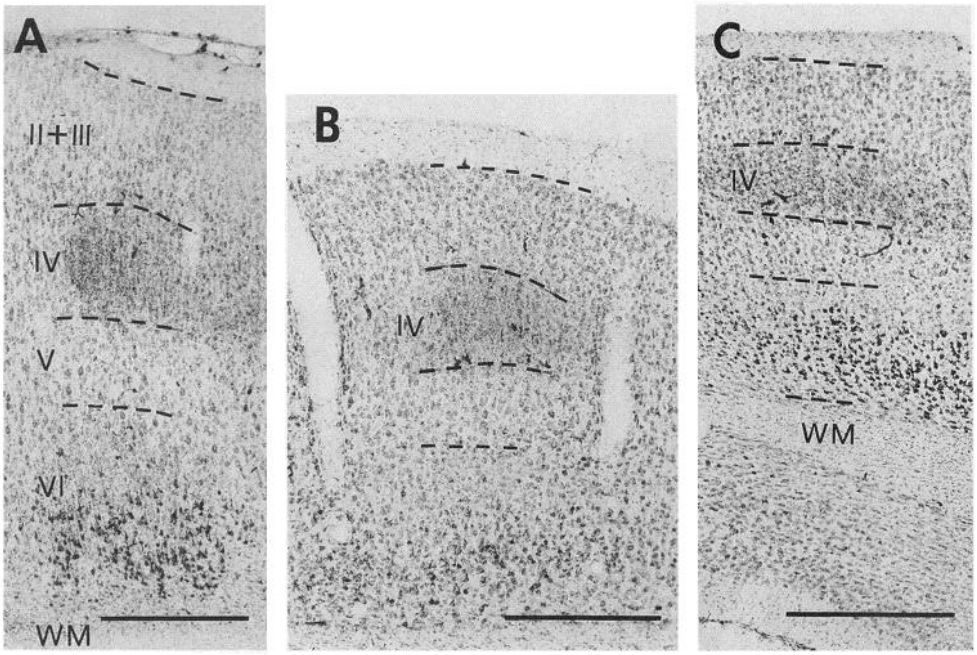

Figure 2. Sections of cortex, processed with TMB/W histochemistry; thionin counterstain. Iontophoretic injections into the corresponding sensory thalamic nuclei resulted in anterograde labeling in layer IV and retrograde labeling in layer VI of S-1 (*A*), A-1 (*B*), or V-1 (*C*). Scale bars, 500 μm.

Electron microscopy

Thalamocortical terminals in layer IV, identified by the presence of electron-dense reaction product (Fig. 4), were usually ovoid, though some had concave appositions. Labeled profiles 0.3–0.5 μm^2 in area were numerous in all three regions of cortex; larger terminals were more common in S-1 than in A-1 or V-1 (Fig. 5*A*, Table 1). Labeled terminals were rich in mitochondria. Terminal area and mitochondrial area were positively correlated. Terminals made asymmetric contacts mainly with spines, often exhibiting multiple active zones interpreted as perforated (Fig. 4*B,D*). Thalamocortical terminals were loosely packed with round, clear vesicles. Some terminals also contained a few dense-core vesicles.

Corticocortical terminals in layer IV labeled after nearby WGA-HRP injections resembled those labeled with CTB-HRP (Fig. 4*E,F*). Most of these corticocortical terminals made asymmetric synaptic contacts and contained small round vesicles; these were selected for systematic study. Like thalamocortical fibers, they terminated mainly on spines, but in other regards they differed markedly (Table 2). They were half the area of thalamocortical terminals (Fig. 5*B*). The electron-dense active zone was large but lacked perforation. These terminals usually lacked mitochondria. Clear vesicles either completely filled the terminal or were densely clustered near the active zone; about 20% also contained dense-core vesicles.

Immunocytochemistry

Glu was detectable in all tissue compartments, presumably reflecting its ubiquitous metabolic functions (Fig. 6*A*). Though this antibody has been thoroughly characterized in previous publications (Hepler et al., 1988; Johansen et al., 1989; Abdullah et al., 1992; Phend et al., 1992), to verify specificity of staining in the present material, we performed additional controls. (1) There was virtually no staining when we substituted preimmune rabbit serum for immune serum (Fig. 6*B*). (2) The reaction was effectively blocked by the addition of exogenous L-glutamate (Fig. 6*C*). Moreover, immunostaining was absent from areas of plastic resin devoid of tissue, such as capillary lumina (Fig. 7*A*). In neuronal somata, Glu immunostaining was concentrated over cytoplasmic organelles, especially mitochondria and rough endoplasmic reticulum; in the nucleus, staining was concentrated over the nucleolus and nuclear heterochromatin. Glu immunostaining was sparse over astrocytic profiles and their mitochondria. Staining in dendrites was variable and concentrated over mitochondria and microtubules. Spines were rich in Glu, especially over the postsynaptic density and the spine apparatus. In synaptic terminals, Glu was concentrated over mitochondria and in vesicle-rich areas. Both axoplasm and mitochondria of identified thalamocortical terminals in all three cortical areas appeared to be enriched in Glu (Figs. 6*A–D*, 7).

To help assess "background" Glu staining, we identified pro-

→

Figure 3. Pattern of labeling in cortex (processed with TMB/W histochemistry). *A*, Posterolateral S-1 (vibrissae representation) after iontophoretic injection targeting VPM. Dense anterograde labeling in layer IV (viewed with crossed polarizers) extended into more superficial layers. *B*, Coronal sections after pressure injection into ventrobasal complex (case shown in Fig. 1*A*). Note patchy organization of labeling throughout S-1, also prominent in S-2. *Numbers* indicate distance from bregma (mm). *C*, Photomontage showing tangential sections through layer IV of S-1, after an injection similar to that in *B* (dark-field illumination); patches of anterograde labeling reveal somatotopic organization of the thalamocortical projection. *av*, anterior vibrissae; *pv*, posterior vibrissae; *fl*, forelimb; *w*, wrist; *hl*, hindlimb. Scale bars: *A*, 500 μm; *B* and *C*, 1 mm.

Figure 4. EM appearance of anterogradely labeled terminals; TMB/W histochemistry. *A*, Low-magnification view of layer IV neuropil after injection of tracer in ventrobasal complex; *arrowheads* show labeled terminals. *B–D*, Higher-magnification views of typical medium to large axospinous synapses made by thalamocortical terminals: *B*, S-1 (vibrissal representation); *C*, V-1; *D*, A-1. After injections of CTB-HRP (*E*) or WGA-HRP (*F*) into cortex, tracer was usually in small terminals. Note the lack of mitochondria in cortical terminals compared with thalamocortical terminals (see also Tables 1, 2). *M*, mitochondrion; *SP*, spine; *V*, synaptic vesicles; *GL*, glial process; *D*, dendrite. Scale bars, 0.5 μm.

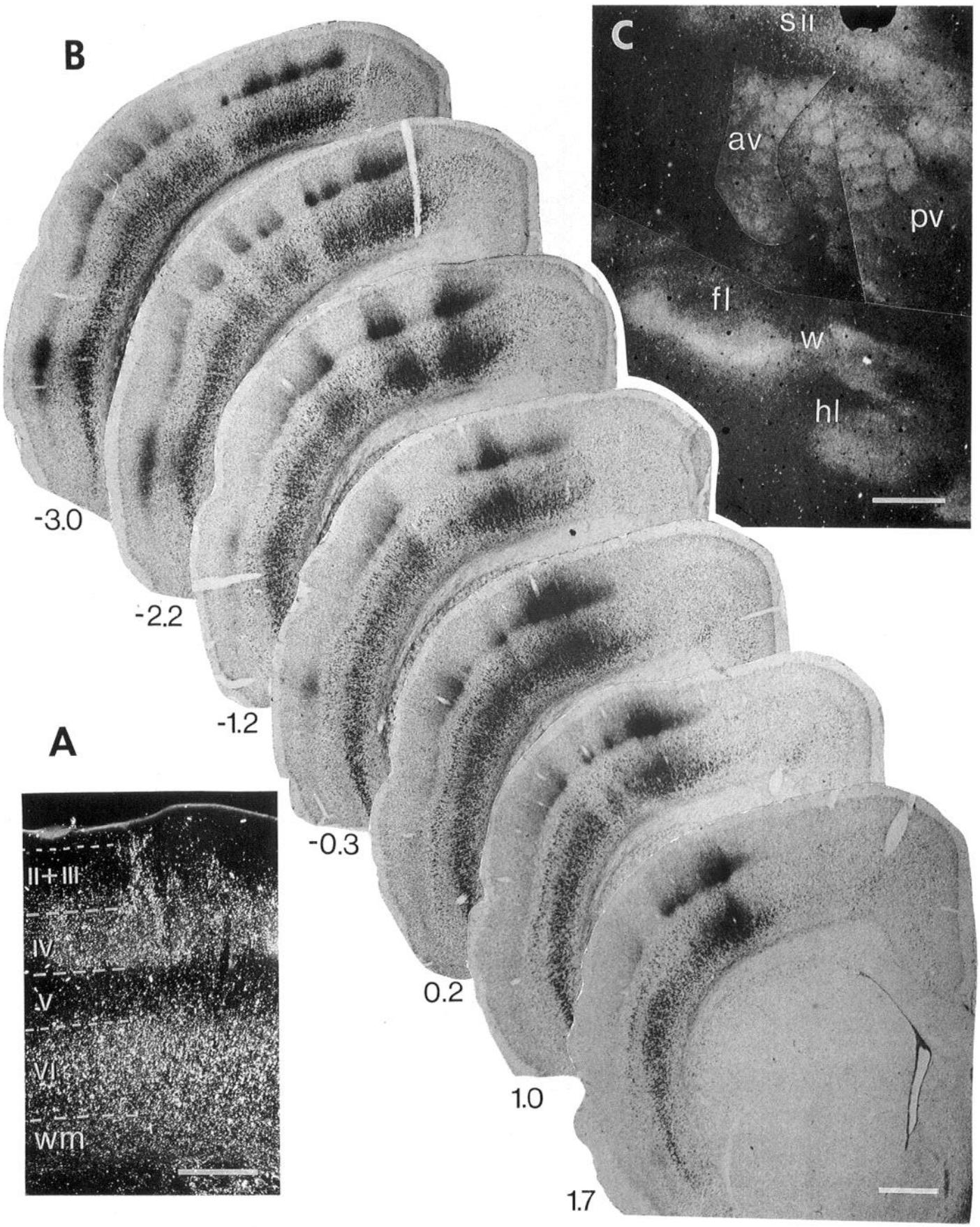
B
C
SII
av
pv
fl
w
hl
-3.0
-2.2
-1.2
-0.3
0.2
1.0
1.7
A
II+III
IV
V
VI
wm

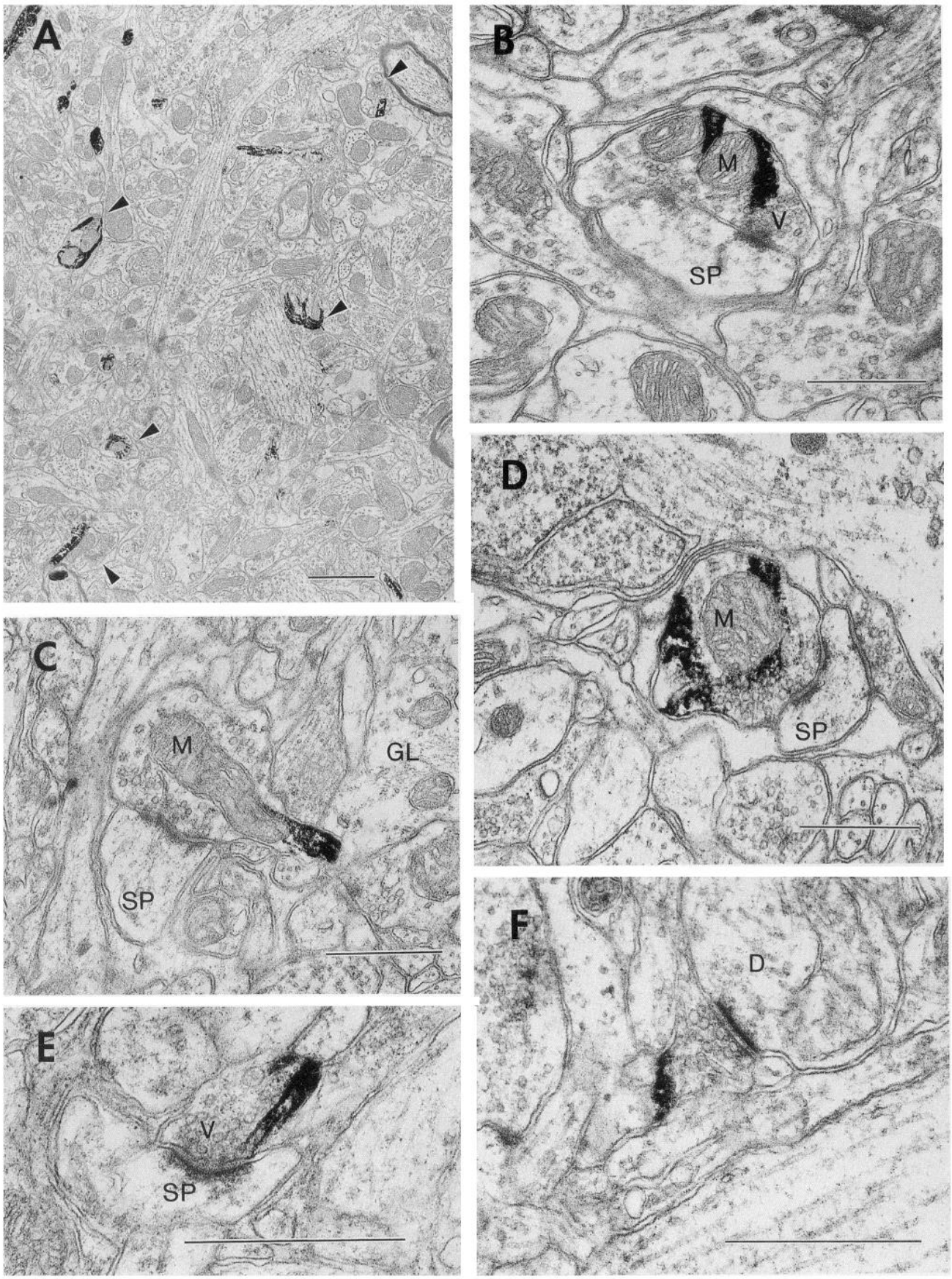
A
B
M
V
SP
C
M
GL
SP
D
M
SP
E
V
SP
F
D

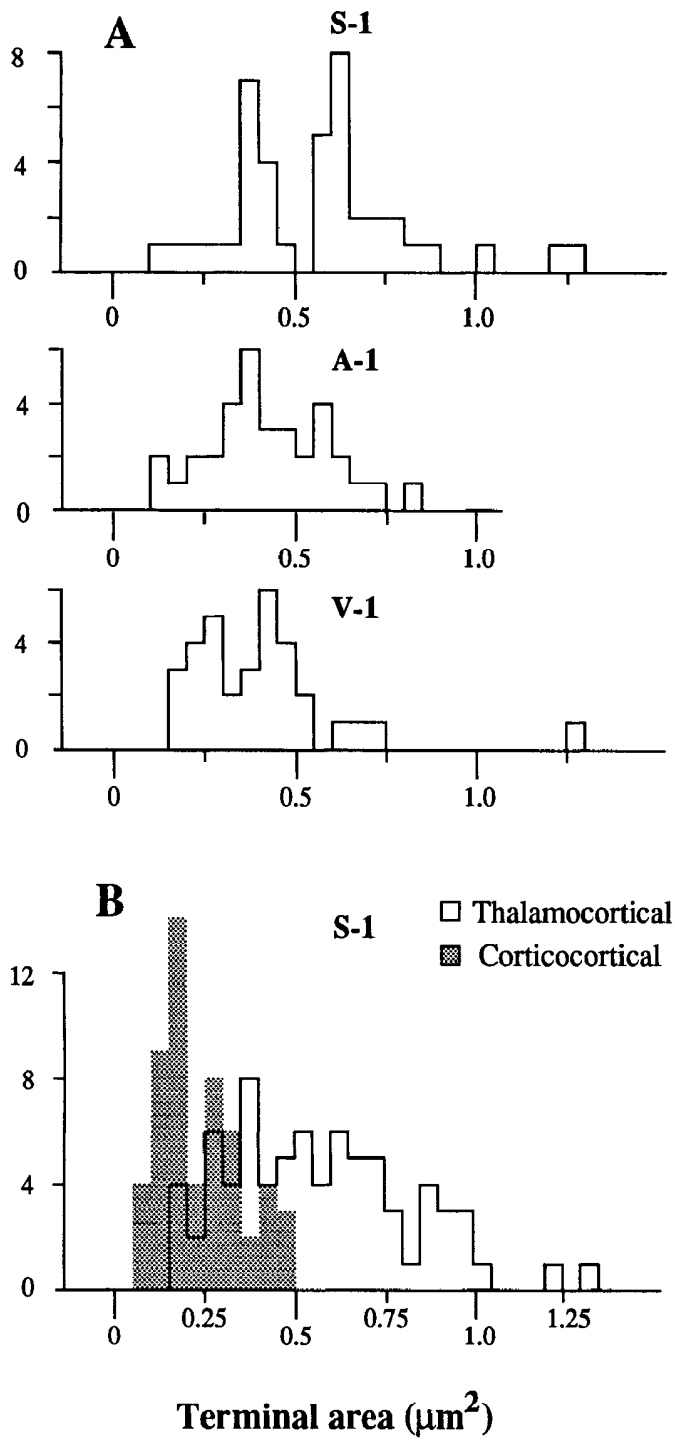

Figure 5. Histograms showing size distribution of HRP-labeled terminals. *A*, Distribution of areas of thalamocortical terminals in S-1 (vibrissal representation), A-1, and V-1. Terminals with area of 0.3–0.5 μm^2 were numerous in all sensory areas; large terminals with area more than 0.6 μm^2 were uncommon in visual cortex and sparser in A-1 than in S-1. *B*, Distribution of areas of labeled thalamocortical and corticocortical terminals sampled in forelimb area of S-1, from two different animals. Corticocortical terminals (*shaded*) were markedly smaller than thalamocortical terminals (see also Table 2).

files rich in GABA. GABA immunostaining was concentrated over a restricted group of somata, aspiny dendrites, axons, and synaptic terminals, interpreted as GABAergic (Fig. 6*D*). Virtually all HRP-labeled somata in layer IV (interpreted as transneuronally labeled) were GABAergic; with EM these could be

Table 1. Thalamocortical terminals in three regions of cortex

	S-1	A-1	V-1
Terminal area (μm^2)	0.57 ± 0.04	0.43 ± 0.03	0.40 ± 0.04
Mitochondrial fraction	0.21 ± 0.02	0.21 ± 0.02	0.23 ± 0.03
Axospinous synapses	91%	94%	93%
Spine area (μm^2)	0.20 ± 0.01	0.17 ± 0.01	0.13 ± 0.01

Data are from photomicrographs of S-1 (52 terminals), A-1 (34 terminals), and V-1 (49 terminals) after iontophoretic injections of WGA-HRP in the thalamus (VPM, ventral medial geniculate, and dorsal lateral geniculate nuclei, respectively). Terminals in all three regions were similar.

seen to receive synapses from labeled thalamocortical terminals. Attention was focused on GABAergic terminals in the same field as thalamocortical terminals. These GABAergic terminals were morphologically similar for all three areas (Table 3). They were as large as thalamic terminals and even richer in mitochondria, making symmetric synapses mainly onto dendritic shafts. They were loosely packed with vesicles, typically small and round. Dense-core vesicles often seemed to be present, but variable electron density of the vesicles made routine identification difficult. GABAergic terminals appeared to be Glu negative, and none of the labeled thalamocortical terminals were immunopositive for GABA.

To establish whether thalamocortical terminals were significantly enriched in Glu, and to define reference levels likely to reflect metabolic Glu pools, we performed quantitative analysis of Glu immunostaining in these terminals, as well as in spines postsynaptic to thalamocortical terminals, random dendrites, GABAergic terminals, and glial processes (Fig. 6*D*). Mitochondria were excluded from computation of these densities. One-way ANOVA revealed highly significant differences in Glu levels for the different types of profiles in all three regions of cortex (S-1, $F = 55.8$; A-1, $F = 41.1$; V-1, $F = 60.5$; all p values < 0.001). For all three sensory systems, levels of Glu in thalamocortical terminals were similar, and significantly higher than those in postsynaptic spines, randomly selected GABA-negative dendrites, GABAergic terminals, or glia (Fig. 8). Glu levels in

Table 2. Thalamocortical and corticocortical terminals

	Thalamocortical	Corticocortical
Terminal area (μm^2)	0.57 ± 0.03	0.24 ± 0.02
Mitochondrial fraction	0.17 ± 0.02	0.04 ± 0.01
Axospinous synapses	92%	91%
Spine area (μm^2)	0.19 ± 0.01	0.16 ± 0.01

Data are from micrographs of S-1 (forelimb representation) after pressure injections in VPL (76 terminals), or in adjacent cortex (54 terminals making asymmetric synapses). Thalamocortical terminals were larger and richer in mitochondria than corticocortical terminals.

Table 3. GABAergic terminals in three regions of cortex

	S-1	A-1	V-1
Terminal area (μm^2)	0.47 ± 0.04	0.44 ± 0.04	0.50 ± 0.04
Mitochondrial fraction	0.27 ± 0.02	0.24 ± 0.02	0.32 ± 0.03

Data are from photomicrographs of S-1 (30 terminals), A-1 (24 terminals), and V-1 (30 terminals) close (< 10 μm) to labeled thalamocortical terminals (from the same material as Table 1). GABAergic terminals were as large as thalamocortical terminals, and contained even more mitochondria.

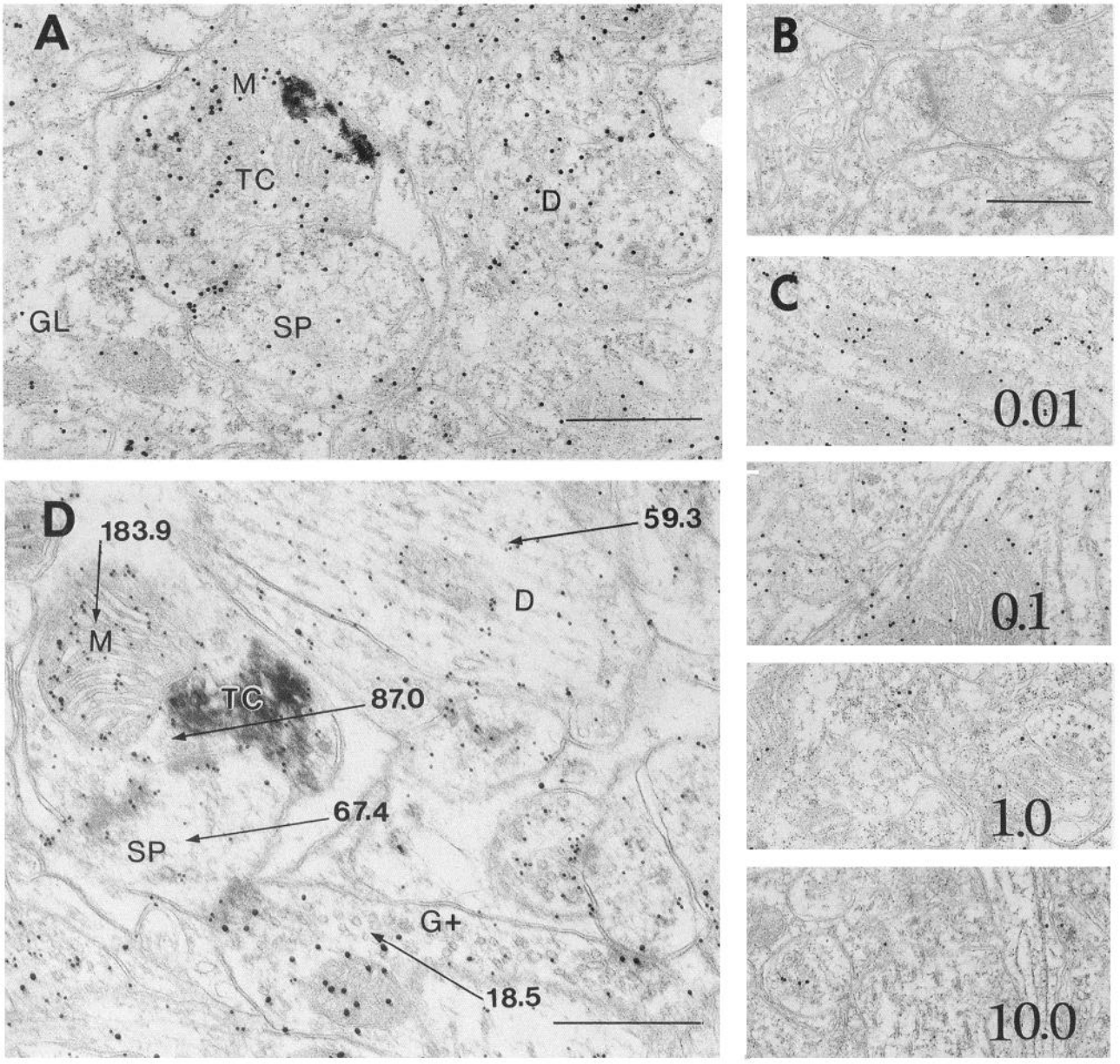

Figure 6. Postembedding immunocytochemistry for Glu. *A,* Section from S-1 immunoreacted for Glu (1:200,000). Though visible over all tissue compartments, gold particles were concentrated over the thalamocortical terminal (*TC*) and regions of the spine (*SP*) immediately postsynaptic to it. Particles were sparse over glia (*GL*), but high over the dendrite (*D*) in this micrograph. *B,* Labeling was virtually absent from another section cut from the same tissue, substituting preimmune rabbit serum (1:100,000) for primary antibody. *C,* Preincubation of antiserum with 0.01 mM Glu (*top panel*) had little effect on immunostaining, but staining was progressively blocked after preincubation in higher concentrations of Glu (*lower panels*). *D,* Material from S-1 after thalamic injection in another animal, double-immunoreacted for Glu (1:200,000; small particles) and GABA (1:10,000; large particles). *Numbers* represent densities of gold particles coding for Glu over various tissue compartments. Glu was concentrated over thalamocortical terminal (*TC*) and especially over mitochondrion within this terminal (*M*). In view of its probable metabolic role in mitochondria, mitochondrial densities of Glu were not considered in the quantitative study. Note low concentration of Glu over GABA-positive terminal (*G+*); spine (*SP*) had higher Glu concentration than dendrite (*D*), due to the high Glu concentration in the region of the postsynaptic density. *A–C,* 20 nm gold particles; *D,* 18 nm gold (*Glu*) and 30 nm gold (*GABA*). Scale bars: 0.5 μm (scale bar in *B* also for *C*).

thalamocortical terminals remained significantly elevated even after making a (very conservative) Bonferroni adjustment for multiple *t* tests. Postsynaptic spines were also significantly enriched in Glu, compared to dendrites. Astrocytic processes had very low levels of Glu.

Glu in thalamocortical terminals appeared elevated in vesicle-containing regions. The quantitative relationship between Glu and synaptic vesicles was studied in a population of layer IV terminals in the vibrissal representation of S-1, from an animal with optimal tissue preservation. Nearby GABAergic terminals were tallied as a control, to verify that Glu density over vesicles was not merely a consequence of the presence of vesicles (e.g., by serving as a passive antigen-retaining structure). There was a significant correlation between Glu density and vesicle density over vesicle-containing regions for identified thalamocortical terminals ($r = 0.57$, $n = 19$; Fig. 9). No significant correlation

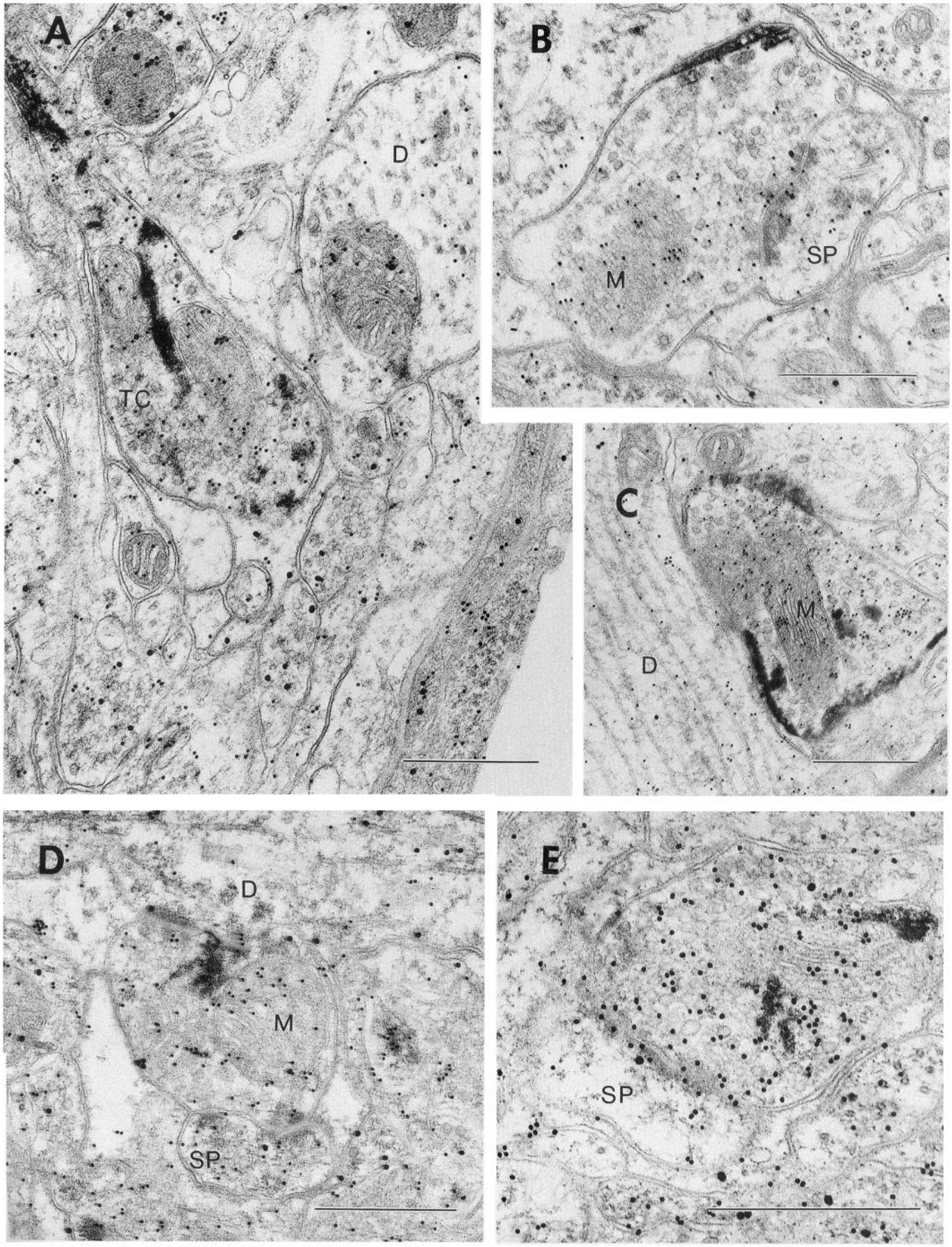
A
D
TC
B
M
SP
C
M
D
D
D
M
SP
E
SP

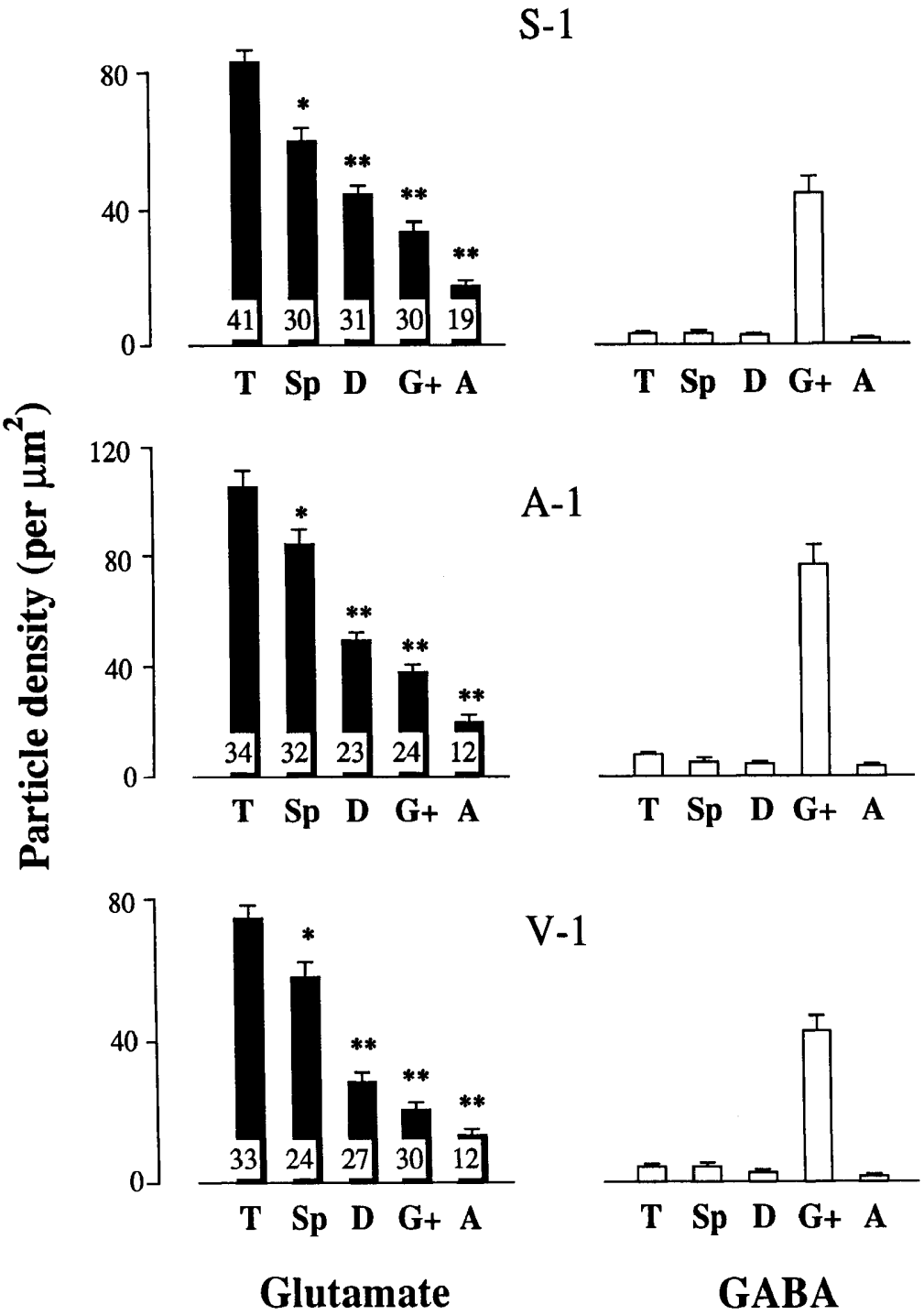

Figure 8. Histograms showing densities of immunostaining for Glu and GABA in three animals with injections in VPM, ventral medial geniculate, and dorsal lateral geniculate, respectively. (These cases were selected for ultrastructural preservation and density of anterograde labeling; similar results were seen in other animals.) Densities of immunostaining were similarly distributed in S-1 (vibrissae), A-1, and V-1; Glu was significantly higher in thalamocortical terminals (*T*) than in dendritic spines (*Sp*), and much higher than in dendrites (*D*), GABAergic terminals (*G+*), or astrocytic processes (*A*). *Number inside bars* is sample size. *, $p < 0.01$; **, $p < 0.001$; two-sided *t* tests. GABAergic terminals had much higher GABA immunostaining than other profiles (*right side*). Immunostaining densities for both Glu and GABA were computed after excluding mitochondria.

was seen for the GABAergic terminals, which were uniformly low in Glu ($r = 0.16$, $n = 22$).

Discussion

Morphological observations

Thalamic fibers terminating in layer IV of different regions of cortex were generally similar, and differed markedly from terminals originating from nearby cortical neurons. Though this difference is suggested by published photomicrographs (Jones and Powell, 1970; Garey and Powell, 1971; LeVay and Gilbert, 1976; Peters and Feldman, 1976; Sloper and Powell, 1978; Hersch and White, 1981; McGuire et al., 1984; White and Keller, 1987; LeVay, 1988; Enhanane and White, 1990; Czeiger and White, 1993), the present study provides morphometric

←

Figure 7. HRP-labeled terminals after double immunoreaction for Glu and GABA. *A–C*, Thalamocortical terminals in S-1 vibrissae representation. *D*, V-1; *E*, A-1. Glu immunostaining (18 nm gold) was concentrated in thalamocortical terminals, compared to other nearby profiles. Mitochondria often exhibited high levels of immunostaining. *TC*, thalamocortical terminal; *D*, dendrite; *M*, mitochondria; *SP*, spine. Scale bars, 0.5 μm.

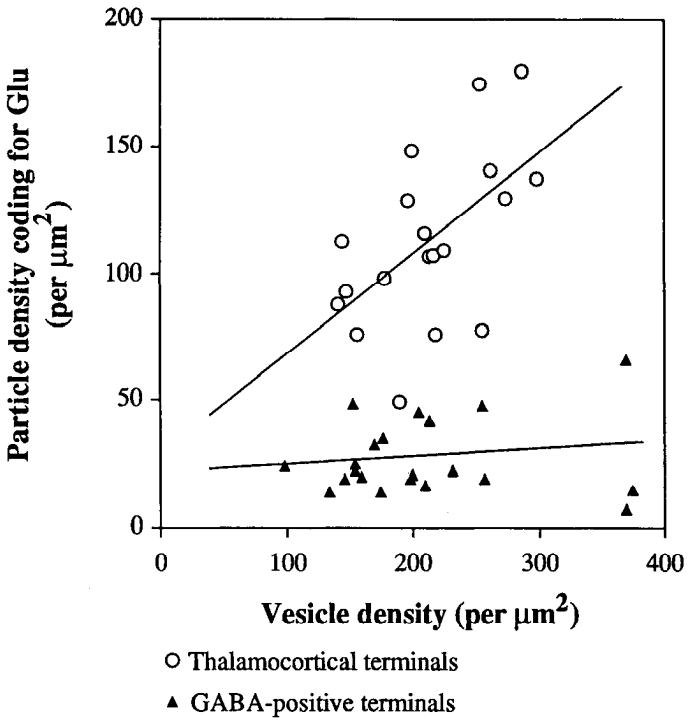

Figure 9. Scatterplot showing Glu immunostaining over vesicle-containing regions in thalamocortical terminals (*circles*) and GABAergic terminals (*triangles*); regression lines are least squares fits. Density of Glu immunostaining in thalamocortical terminals was significantly correlated with the density of synaptic vesicles; there was no significant correlation between Glu and synaptic vesicles in GABAergic terminals.

documentation of differences in these two classes of terminals. Retrograde labeling of corticothalamic neurons was prominent in our material; it is thus in principle possible that some of the layer IV terminals seen after thalamic injection were ascending collaterals of these corticothalamic neurons. However, in view of the clear morphological differences between terminals labeled after thalamic injections and after injections in cortex, we consider it unlikely that a significant fraction of labeled terminals were of cortical origin.

Among the differences between terminals labeled after thalamic versus cortical injections, the larger size of thalamocortical than corticocortical terminals was striking. Though the functional significance of terminal size remains unclear, large terminals are associated with strong synaptic drive (e.g., neuromuscular junction, sympathetic ganglia, dorsal column nuclei, ventral cochlear nucleus; see Pierce and Lewin, 1994, for further discussion). This possibility is consistent with electrophysiological evidence that thalamocortical synaptic drive may be very strong (Hellweg et al. 1977). The modest difference in size between thalamocortical terminals in the three areas is unlikely to arise from differential shrinkage, since GABA terminals in the three regions were of uniform size. We speculate that the larger size and denser termination of thalamocortical terminals in S-1 (especially in the vibrissal representation) compared to the smaller terminals in A-1 and V-1 may be a specialization related to the relative importance of the various sensory modalities in the life of the rat (Vincent, 1912; Krieg, 1946; Stein and Meredith, 1993). The greater mitochondrial fraction in thalamocortical terminals suggests that thalamocortical neurons may have a higher mean firing rate than corticocortical neurons (see review by Wong-Riley, 1989), as suggested also by electrophysiological data (Simons and Carvell, 1989). This mitochondrial enrichment of thalamocortical terminals in layer IV is consistent with previous studies correlating regions of thalamic termination in cortex with elevated levels of oxidative metabolism (Fried, 1966; Killackey and Belford, 1979; Jensen and Killackey, 1987).

Glutamate as a thalamocortical transmitter

Glutamate was significantly enriched in thalamocortical terminals, in comparison with other profiles; the level of this enrichment was comparable in all three cortical areas. Thalamocortical terminals with large areas had concentrations of Glu at least as high as those with relatively small areas (a population that might have been "contaminated" by retrogradely labeled corticothalamic neurons; see above and Fig. 5*B*). Similarly, thalamocortical terminals with large mitochondrial fractions had densities of Glu comparable to those with relatively small mitochondrial fractions (thus, exclusion of mitochondria from computations of particle density did not significantly affect the result).

Immunostaining in other profiles is likely also to represent Glu, rather than some nonspecific staining artifact, since (1) the antiserum has low cross-reactivity to other chemicals found in significant concentrations in tissue (Hepler et al., 1988; Johansen et al., 1989; Abdullah et al., 1992), (2) virtually no particles were seen over areas of plastic devoid of tissue, and (3) staining was blocked similarly over all profiles by preincubation with Glu (see Fig. 6*C*). Gold particle density exhibits an approximately linear relationship with Glu at moderate Glu concentrations (Ottersen, 1989), but higher Glu concentrations may show lower particle density than would be predicted by linearity (Broman and Ottersen, 1992), probably reflecting both steric hindrance and the inability of fixation to retain Glu during the immunocytochemical processing at the ≥50 mM concentrations likely to be present in vesicles *in vivo* (Burger et al., 1989). Thus, the true enrichment of Glu in thalamocortical terminals compared to other profiles may be greater than indicated by the histograms.

Low levels of Glu in GABAergic neurons and astrocytes have been previously reported (Ottersen and Storm-Mathisen, 1984; Somogyi et al., 1986; Ji et al., 1991; Broman and Ottersen, 1992; Ottersen et al., 1992; Kharazia and Weinberg, 1993). We interpret Glu levels in GABAergic terminals as a measure of metabolic Glu in synaptic terminals. Since Glu is a GABA precursor, high glutamic acid decarboxylase activity in these terminals might depress Glu below "background." On the other hand, since these terminals require Glu to synthesize their transmitter, Glu levels might be predicted equally well on a priori grounds to be above "background" (see Martin and Rimwall, 1993, for further discussion). It is likely that the low Glu level in astrocytes (believed to play an important role in glutamate uptake) reflects its rapid conversion, via glutamine synthetase, for subsequent neuronal recycling (see reviews by Hertz, 1979; Erecinska and Silver, 1990).

Glu was significantly enriched in thalamocortical terminals in comparison both to randomly selected dendrites and to dendritic spines. The higher levels of Glu in spines postsynaptic to these terminals than in random dendrites raises the possibility that Glu released from terminals may be taken up by the postsynaptic membrane. Postsynaptic Glu uptake into cortical neurons might explain the weak retrograde transport of ^{3}H-D-Asp

to thalamus reported after cortical injections (Ottersen et al., 1983; Barbaresi et al., 1987).

No obvious clustering of gold particles was seen over individual vesicles in the present study, or in previous reports of postembedding immunocytochemistry for amino acid neurotransmitters. That this does not reflect the limited spatial resolution of the immunogold method is indicated by previous reports showing immunolabeling for neuropeptides over dense-core vesicles (De Biasi and Rustioni, 1988). There are several possible explanations for this less restrictive labeling: (1) the clear synaptic vesicles are so small that most are unlikely to be fully accessible to the antibody; (2) there may be *in vivo* differences in the relative concentrations of the two classes of neuromediators in different synaptic compartments, and intravesicular amino acid concentrations are likely to be in the nonlinear range for the immunogold method; (3) since peptides are easier to fix than amino acids, and large dense-core vesicles seem to be more stable than clear round vesicles, peptides are likely to exhibit less postmortem diffusion than amino acids. Nevertheless, a relationship between Glu enrichment and synaptic vesicle density has been reported (Ji et al., 1991). In the present study, the strong positive correlation between Glu labeling and vesicle density in these terminals and the lack of such a correlation in GABAergic terminals lend further support to the notion that these terminals are likely to use Glu as a neurotransmitter.

Glu receptor antagonists can block thalamic excitation of layer IV neurons, and Glu is released in a Ca^{2+}-dependent fashion after thalamic stimulation (Tamura et al., 1990; Hicks et al., 1991). This evidence is not conclusive (see the introductory remarks) since it does not clearly distinguish thalamocortical from corticocortical pathways. The present results strongly support the hypothesis that thalamocortical neurons to S-1 and V-1 use Glu as a neurotransmitter, since our anatomical observations provide direct evidence of its presence in the terminal. Considering the very similar levels of Glu in thalamic terminals to all three regions, it is probable that Glu is a thalamocortical neurotransmitter also for A-1. While the present results do not exclude that other substances, including large neuropeptides, dipeptides such as *N*-acetylaspartylglutamate, and/or aspartate may also play a role, we propose that Glu may be the main thalamocortical neurotransmitter to all regions of cortex.

References

Abdullah LH, Ordronneau P, Petrusz P (1992) Molecular requirements for hapten binding to antibodies against glutamate and aspartate. Neuroscience 51:729–738.

Barbaresi P, Fabri M, Conti F, Manzoni T (1987) D[^{3}H]aspartate retrograde labelling of callosal and association neurones of somatosensory areas I and II of cats. J Comp Neurol 263:159–178.

Brodmann K (1909) Vergleichende Lokalisationslehre der Grosshirnrinde in Ihren Prinzipien dargestellt auf Grund des Zellenbaues. Leipzig: Barth.

Broman J, Ottersen OP (1992) Cervicothalamic tract terminals are enriched in glutamate-like immunoreactivity: an electron microscopic double-labeling study in the cat. J Neurosci 12:204–221.

Burger PM, Mehl E, Cameron PL, Maycox PR, Baumert M, Lottspeich F, De Camilli P, Jahn R (1989) Synaptic vesicles immunoisolated from rat cerebral cortex contain high levels of glutamate. Neuron 3:715–720.

Conti F, Rustioni A, Petrusz P, Towle AC (1987) Glutamate-positive neurons in the somatic sensory cortex of rats and monkeys. J Neurosci 7:1887–1901.

Conti F, DeFelipe J, Farinas I, Manzoni T (1989) Glutamate-positive neurons and axon terminals in cat sensory cortex: a correlative light and electron microscopic study. J Comp Neurol 290:141–153.

Czeiger D, White EL (1993) Synapses of extrinsic and intrinsic origin made by callosal projection neurons in mouse visual cortex. J Comp Neurol 330:502–513.

DeBiasi S, Rustioni A (1988) Glutamate and substance P coexist in primary afferent terminals in the superficial laminae of spinal cord. Proc Natl Acad Sci USA 85:7820–7824.

Enhanane E, White E (1990) Intrinsic circuitry: synapses involving the local axon collaterals of corticocortical projection neurons in the mouse primary somatosensory cortex. J Comp Neurol 291:43–54.

Erecinska M, Silver IA (1990) Metabolism and role of glutamate in mammalian brain. Prog Neurobiol 35:245–296.

Fried RL (1966) Topographic brain chemistry. New York: Academic.

Garey LJ, Powell TPS (1971) An experimental study of the termination of the lateral geniculo-cortical pathway in the cat and monkey. Proc R Soc Lond [Biol] 179:41–63.

Giuffrida R, Rustioni A (1989) Glutamate and aspartate immunoreactivity in cortico-cortical neurons of the sensorimotor cortex of rats. Exp Brain Res 74:41–46.

Hellweg F-C, Schultz W, Creutzfeldt OD (1977) Extracellular and intracellular recording from cat's cortical whisker projection area: thalamocortical response transformation. J Neurophysiol 40:463–479.

Hepler JR, Toomim CS, McCarthy KD, Conti F, Battaglia G, Rustioni A, Petrusz P (1988) Characterization of antisera to glutamate and aspartate. J Histochem Cytochem 36:13–22.

Herkenham M (1980) Laminar organization of thalamic projections to the rat neocortex. Science 207:532–535.

Herkenham M (1986) New perspectives on the organization and evolution of nonspecific thalamocortical projections. In: Cerebral cortex, Vol 5, Sensory-motor areas and aspects of cortical connectivity (Jones EG, Peters A, eds), pp 403–445. New York: Plenum.

Hersch SM, White EL (1981) Thalamocortical synapses involving identified neurons in mouse primary somatosensory cortex: a terminal degeneration and Golgi/EM study. J Comp Neurol 195:253–263.

Hertz L (1979) Functional interactions between neurons and astrocytes. I. Turnover and metabolism of putative amino acid transmitters. Prog Neurobiol 13:277–323.

Hicks TP, Kaneko T, Metherate R, Oka J-I, Stark X (1991) Amino acids as transmitters of synaptic excitation in neocortical sensory processes. Can J Physiol Pharmacol 69:1099–1114.

Jensen KF, Killackey HP (1987) Terminal arbors of axons projecting to the somatosensory cortex of the adult rat. I. The normal morphology of specific thalamocortical afferents. J Neurosci 7:3529–3543.

Ji Z, Aas JE, Laake J, Walberg F, Ottersen OP (1991) An electron microscopic, immunogold analysis of glutamate and glutamine in terminals of rat spinocerebellar fibers. J Comp Neurol 307:296–310.

Johansen J, Halpern ME, Johansen KM, Keshishian H (1989) Stereotypic morphology of glutamatergic synapses on identified muscle cells of *Drosophila* larvae. J Neurosci 9:710–725.

Johnson RR, Burkhalter A (1992) Evidence for excitatory amino acid neurotransmitters in the geniculo-cortical pathway and local projections within rat primary visual cortex. Exp Brain Res 89:20–30.

Jones EG (1981) Anatomy of cerebral cortex: columnar input-output organization. In: The organization of cerebral cortex (Schmitt FO, Worden FG, Edelman G, Dennis SG, eds), pp 199–235. Cambridge, MA: MIT Press.

Jones EG (1985) The thalamus, p 244. New York: Plenum.

Jones EG (1988) Modern views of cellular thalamic mechanisms. In: Cellular thalamic mechanisms (Bentivoglio M, Spreafico R, eds), pp 1–22. Amsterdam: Elsevier.

Jones EG, Powell TPS (1970) An electron microscopic study of terminal degeneration in the neocortex of the cat. Philos Trans R Soc Lond [Biol] 257:29–43.

Kemper TLB, Galaburda AM (1984) Principles of cytoarchitectonics. In: Cerebral cortex, Vol 1, Cellular components of the cerebral cortex (Peters A, Jones EG, eds), pp 35–57. New York: Plenum.

Kharazia VN, Weinberg RJ (1993) Glutamate in terminals of thalamocortical fibers in rat somatic sensory cortex. Neurosci Lett 157: 162–166.

Killackey HP, Belford GR (1979) The formation of afferent patterns in the somatosensory cortex of the neonatal rat. J Comp Neurol 183: 285–304.

Krieg WJS (1946) Connections of the cerebral cortex. I. The albino rat. B. Structure of the cortical areas. J Comp Neurol 84:277–323.

LeVay S (1988) Patchy intrinsic projection in visual cortex, area 18, of the cat: morphological and immunocytochemical evidence for excitatory function. J Comp Neurol 269:265–274.

LeVay S, Gilbert C (1976) Laminar pattern of geniculocortical projection in the cat. Brain Res 113:1–19.
Martin DL, Rimvall KJ (1993) Regulation of γ-aminobutyric acid synthesis in the brain. Neurochemistry 60:395–407.
McCormick DA (1992) Neurotransmitter actions in the thalamus and cerebral cortex and their role in neuromodulation of thalamocortical activity. Prog Neurobiol 39:337–388.
McGuire BA, Horning J-P, Gilbert C, Wiesel TN (1984) Patterns of synaptic input to layer 4 of cat striate cortex. J Neurosci 4:3021–3033.
Montero VM (1990) Quantitative immunogold analysis reveals high glutamate levels in synaptic terminals of retino-geniculate, cortico-geniculate, and geniculo-cortical axons in the cat. Vis Neurosci 4:437–443.
Orrego F, Villanueva S (1993) The chemical nature of the main central excitatory transmitter: a critical appraisal based upon release studies and synaptic vesicle localization. Neuroscience 56:539–556.
Ottersen OP (1989) Post-embedding immunogold labeling of fixed glutamate: an electron microscopic analysis of the relationship between gold particles density and antigen concentration. J Chem Neuroanat 2:57–66.
Ottersen OP, Storm-Mathisen J (1984) Glutamate- and GABA-containing neurons in the mouse and rat brain, as demonstrated with a new immunocytochemical technique. J Comp Neurol 229:374–392.
Ottersen OP, Fischer B, Storm-Mathisen J (1983) Retrograde transport of D-[^{3}H]aspartate in thalamocortical neurones. Neurosci Lett 42:19–24.
Ottersen OP, Zhang N, Walberg F (1992) Metabolic compartmentation of glutamate and glutamine: morphological evidence obtained by quantitative immunocytochemistry in rat cerebellum. Neuroscience 46:519–534.
Paxinos G, Watson C (1986) The rat brain in stereotaxic coordinates. Orlando, FL: Academic.
Peters A, Feldman M (1976) The projection of the lateral geniculate nucleus to area of the rat cerebral cortex. I. General description. J Neurocytol 5:63–84.
Peters A, Palay SL, Webster H DeF (1991) The fine structure of the nervous system, 3d ed. New York: Oxford UP.
Phend KD, Weinberg RJ, Rustioni A (1992) Techniques to optimize post-embedding single and double staining for amino acid neurotransmitters. J Histochem Cytochem 40:1011–1020.
Pierce JP, Lewin GR (1994) An ultrastructural size principle. Neuroscience 58:441–446.
Rustioni A, Battaglia G, De Biasi S, Giuffrida R (1988) Neuromediators in somatosensory thalamus: an immunocytochemical overview. In: Cellular thalamic mechanisms (Bentivoglio M, Spreafico R, eds), pp 311–320. Amsterdam: Elsevier.
Simons DJ, Carvell GE (1989) Thalamocortical response transformation in the rat vibrissa/barrel system. J Neurophysiol 61:311–330.
Sloper JJ, Powell TPS (1978) An experimental electron microscope study of afferent connections to the primate motor and somatic sensory cortices. Philos Trans R Soc Lond [Biol] 285:199–226.
Somogyi P, Halasy K, Somogyi J, Storm-Mathisen J, Ottersen OP (1986) Quantification of immunogold labelling reveals enrichment of glutamate in mossy and parallel fibre terminals in cat cerebellum. Neuroscience 19:1045–1050.
Stein BE, Meredith MA (1993) The merging of the senses. Cambridge, MA: MIT Press.
Streit P (1984) Glutamate and aspartate as transmitter candidates for systems of the cerebral cortex. In: Cerebral cortex, Vol 2, Functional properties of cortical cells (Jones EG, Peters A, eds), pp 119–136. New York: Plenum.
Tamura H, Hicks TP, Hata Y, Tsumoto T, Yamatodani A (1990) Release of glutamate and aspartate from the visual cortex of the cat following activation of afferent pathways. Exp Brain Res 80:447–455.
Tieman SB, Neale JH, Tieman DG (1991) *N*-acetylaspartylglutamate immunoreactivity in neurons of the monkey's visual pathway. J Comp Neurol 313:45–64.
Tsumoto T (1990) Excitatory amino acid transmitters and their receptors in neural circuits of the cerebral cortex. Neurosci Res 9:79–102.
Vincent SB (1912) The function of the vibrissae in the behavior of the white rat. Behav Monogr 1:1–81.
Weinberg RJ, Van Eyck SL (1991) A tetramethylbenzidine/tungstate reaction for horseradish peroxidase histochemistry. J Histochem Cytochem 39:1143–1148.
White E, Keller A (1987) Intrinsic circuitry involving the local axon collaterals of corticothalamic projection cells in mouse SmI cortex. J Comp Neurol 262:13–26.
Wong-Riley MTT (1989) Cytochrome oxidase: an endogenous metabolic marker for neuronal activity. Trends Neurosci 12:94–101.
Xing LC, Tieman SB (1993) Relay cells, not interneurons, of cat's lateral geniculate nucleus contain *N*-acetylaspartylglutamate. J Comp Neurol 330:272–285.